Bone 103 (2017) 55–63

Contents lists available at ScienceDirect

Bone

journal homepage: www.elsevier.com/locate/bone

Full Length Article

Phosphoproteome analysis reveals a critical role for hedgehog signalling in osteoblast morphological transitions

Ariane Marumoto [a], Renato Milani [b], Rodrigo A. da Silva [a], Célio Junior da Costa Fernandes [a], José Mauro Granjeiro [c], Carmen V. Ferreira [b], Maikel P. Peppelenbosch [d], Willian F. Zambuzzi [a,*]

[a] Lab. de Bioensaios e Dinâmica Celular, Depto de Química e Bioquímica, Instituto de Biociências, Universidade Estadual Paulista - UNESP, campus Botucatu, São Paulo 18618-970, Brazil
[b] Laboratory of Bioassays and Signal Transduction, Departamento de Bioquímica, Instituto de Biologia, Universidade Estadual de Campinas (Unicamp), C.P. 6109, CEP 13083-970 Campinas, São Paulo, Brazil
[c] Instituto Nacional de Metrologia, Normalização e Qualidade Industrial (INMETRO), Life Sciences Applied Metrology (Dimav)/Bioengineering Group, Xerém, RJ, Brazil
[d] Erasmus MC Cancer Institute, Erasmus MC, Erasmus University of Rotterdam, Rotterdam, The Netherlands

ARTICLE INFO

Article history:
Received 30 June 2016
Revised 8 June 2017
Accepted 15 June 2017
Available online 17 June 2017

Keywords:
Osteoblast
Sonic Hedgehog
ECM
Biomaterials
Bioengineering

ABSTRACT

The reciprocal and adaptive interactions between cells and substrates governing morphological transitions in the osteoblast compartment remain largely obscure. Here we show that osteoblast cultured in basement membrane matrix (Matrigel™) exhibits significant morphological changes after ten days of culture, and we decided to exploit this situation to investigate the molecular mechanisms responsible for guiding osteoblast morphological transitions. As almost all aspects of cellular physiology are under control of kinases, we generated more or less comprehensive cellular kinome profiles employing PepChip peptide arrays that contain over 1000 consensus substrates of kinase peptide. The results obtained were used to construct interactomes, and these revealed an important role for FoxO in mediating morphological changes of osteoblast, which was validated by Western blot technology when FoxO was significantly up-expressed in response to Matrigel™. As FoxO is a critical protein in canonical hedgehog signalling, we decided to explore the possible involvement of hedgehog signalling during osteoblast morphological changes. It appeared that osteoblast culture in Matrigel™ stimulates release of a substantial amounts Shh while concomitantly inducing upregulation of the expression of the *bona fide* hedgehog target genes Gli-1 and Patched. Functional confirmation of the relevance of these results for osteoblast morphological transitions came from experiments in which Shh hedgehog signalling was inhibited using the well-established pathway inhibitor cyclopamine (Cyc). In the presence of Cyc, culture of osteoblasts in Matrigel™ is not capable of inducing morphological changes but appears to provoke a proliferative response as evident from the upregulation of Cyclin D3 and cdk4. The most straightforward interpretation of our results is that hedgehog signalling is both necessary and sufficient for membrane matrix-based morphological transitions.

1. Introduction

The extracellular matrix (ECM) is a set of important components essential for tissue integrity with some cell types, such as chondrocytes, osteocytes, and fibroblasts, which are more-or-less completely embedded in it [1–3]. The matrix is highly biologically active and provides ligands that regulate cell-matrix interaction. It also provides important cues with respect to cell plasticity and tissue remodelling [2,4]. The details of the interaction between the ECM and the cells that interact with it are still only partly understood. Our knowledge in this area, however, has been substantially bolstered by the discovery that ECM-based scaffolds are useful tools to analyse both physiology and pathophysiology of cell-matrix interactions [1,4,5]. Increasing insight into the molecular mechanisms involved might revolutionise the pursuit of better biomaterials for combating disease, especially in the quest to improve bone regeneration.

Cellular reaction to the extracellular matrix involves complex signal transduction pathways. Almost all of these pathways involve tyrosine kinases and/or serine/threonine kinases (both receptor type and non-receptor type enzymes), which often operate in intricate signalling cascades that defy analysis using conventional technology. The specific importance of phosphorylation derives from the substantial conformational changes in proteins when the negative phosphate group is introduced into the amino acid chain, which allows fast and reversible regulation of protein function, including enzymatic activity. Classically, the study of different kinases or cellular pathways is typically pursued one protein at the time through Western blotting technology, a fairly

* Corresponding author at: Laboratório de Bioensaios e Dinâmica Celular, Depto de Química e Bioquímica Instituto de Biociências – IBB, Universidade Estadual Paulista - UNESP, Brazil.
E-mail address: wzambuzzi@ibb.unesp.br (W.F. Zambuzzi).

http://dx.doi.org/10.1016/j.bone.2017.06.012
8756-3282/

labour-intensive tool, which hampers the generation of comprehensive description of cellular signalling [6,7]. However, advent of kinome profiling has improved this situation. Multiple technologies exist, but especially peptide arrays allow simultaneous analysis of kinase enzymatic activity of 1000 substrates or more in a single experiment [8–10]. This powerful approach has, however, not been exploited to obtain insight into the biochemical pathways that regulate osteoblast phenotype during its interaction with the ECM.

In this study, we documented that pre-osteoblasts cultured on basement membrane matrix (MATRIGEL™) up to 10 days triggers a morphological transition, then, we explored the global kinase profile associated with this event. The profiles obtained suggest an important role for Shh signalling in these changes, mediating morphological change and exit from the cell cycle, which was confirmed when tested directly. These results open new avenues to understand morphological changes of osteoblast at a molecular level and provide a wealth of data on osteoblast adaptation to organic matrix-based substrates. Thus, this study may be useful for the rational design of therapeutic devices.

2. Material and methods

2.1. Reagents, antibodies, and primers

Cyclopamine, β-glycerophosphate, ascorbate, *p*-nitrophenyl-phosphate (*p*NPP), and DMSO were purchased from Sigma Chemical Co (St. Louis, MO, USA); A10490 - MEM alpha, nucleosides, with no ascorbic acid, was from Invitrogen; MATRIGEL™ and recombinant-Sonic Hedgehog (rShh) were from R&D (R&D Systems Inc., Minneapolis). MTT [3-(4,5-dimethylthiazol-2-yl)-2,5-diphenyltetrazolium bromide] was from Calbiochem (Calbiochem, San Diego, CA, USA). The general cell culture supplies were purchased from Bio-One (Greiner Bio-One, Germany). The immunoblotting reagents were purchased from Millipore (Millipore Corporate Headquarters, Billerica, MA, USA). Antibodies: CDK6 (DCS83) mouse mAb #3136; CDK6 #3136; $p21^{Waf1/Cip1}$ #2946; phospho-PI3 kinase p85 (Tyr458)/p55 (Tyr199) #4228; phospho-Akt (Ser473) #4060; PDK1 #5662; GSK-3β #12456; phospho-PKC (pan) (zeta Thr410) #2060; PKA #3927; p38 MAPK #8690; phospho-p44/42 MAPK (Erk1/2) (Thr202/Tyr204) #4370; phospho-Src Family (Tyr416) #6943; phospho-Paxillin (Tyr118) antibody #2541; Shh antibody #2287; Connexin 43 antibody #3512; FoxO1 #2880; phospho-FoxO3a (Ser253) #9466; phospho-FoxO3a (Ser318) #9465; GADPH #5174; anti-mouse IgG, HRP-linked antibody #7076; and anti-rabbit IgG, HRP-linked antibody #7074 were purchased from Cell Signalling Technology (Boston, MA, USA). Patched (C-20; #6147) and β-Actin (C-4; #sc-47778) were from Santa Cruz Biotechnology Inc. (Santa Cruz, CA, USA). Anti-CyclinD1 (C5588) was from Sigma Chemical Co (St. Louis, MO, USA). Primers were obtained from Invitrogen (Breda, Netherlands) and details are listed in Table 1.

2.2. Cell culture and osteoblast morphological change acquisition protocol

MC3T3-E1 (subclone 4), a calvaria mouse pre-osteoblast cell line, was obtained from the ATCC (Manassas, USA) and grown at 37 °C in α-MEM medium supplemented with 10% Foetal Bovine Serum (FBS), 100 U/ml of penicillin, and 100 μg/ml of streptomycin under a humidified 5% CO_2 atmosphere. When appropriate, cells were exposed to osteogenic conditions, which involved α-MEM plus β-glycerophosphate (10 mM) plus ascorbate (50 μg/mL). Before experimentation, a gel was prepared by mixing Matrigel™: α-MEM (2:1), as it was used for coating Petri dishes (100 mm diameter) or 6-wells plates, exactly as indicated by the manufacturer. These petri dishes (or plates) were kept at 37 °C for 3 h prior to each experiment in order to allow MATRIGEL™ gelation. Afterwards, cells were seeded (3×10^4 cells/mL) and cultured for 10 days. The medium was freshly replaced every 3 days. In this protocol, 3 experimental conditions were routinely assayed: 1) osteoblasts cultured on polystyrene (conventional cell culture staffs); 2) cells cultured on MATRIGEL™ as ECM-based scaffold; 3) osteoblast cultured on MATRIGEL, but subjected to osteoblast-differentiation condition (as detailed previously).

Table 1
RT-PCR primers.

Primers		
Gene	Forward	Reverse
Alkaline phosphatase (ALP)	5′-aacccagacacaagcattcc-3′	5′-cgaagggtcagtcaggttgt-3′
Osteocalcin (OCN)	5′-gcgctctgtctctctgacct-3′	5′-gccggagtctgttcactacc-3′
Cathepsins B (CtsB)	5′-tgcatcctagcctctcccta-3′	5′-ggaagtcctgcagtcaaagc-3′
Cathepsins K (CtsK)	5′-tctctcggcgtttaatttgg-3′	5′-aagtggttcatggccagttc-3′
β-Actin	5′-cctaaggccaaccgtgaaaag-3′	5′-tcttcatggtgctaggagcca-3′

2.3. Treatment with recombinant Shh (rShh) or cyclopamine (Cyc)

In order to confirm whether hedgehog signalling was able to promote osteoblast morphological change, we treated pre-osteoblasts with rShh or cyclopamine (Shh inhibitor) for up to 6 days. Before experimentation, the gel-mix was prepared as described before, but either rShh (10 ng/mL) or cyclopamine (2 μM) was included in the mixture as appropriate, and this gel-mix was used to coat Petri dishes (100 mm) or 6-wells plates. Cyc at the concentration used here did not induce cytotoxicity (data not shown). Coated dishes were incubated at 37 °C for 3 h before seeding 3×10^4 cells/mL and cultured for 6 days. Results were analysed using a Leica microscope/camera and the samples were collected for Western blotting. Medium was replaced every 3 days.

2.4. Cellular viability assay

In order to check the cell viability, MC3T3-E1 cells (3×10^4 cells/mL) were seeded consistent with the appropriate experimental condition in 24-wells plates and maintained for 10 days. Afterwards, the medium was removed and 1 mL (1 mg/mL) of 3-(4,5-dimethylthiazol-2-yl)-2,5-diphenyltetrazolium bromide (MTT) was added to each well [11]. After 4 h of incubation at 37 °C, the medium was removed and the reduced formazan was solubilised in 1 mL of DMSO (Sigma-Aldrich, USA). Then, the plate was shaken for 10 min on a plate shaker (Biotek, Winooski, VT, USA) and the absorbance was measured at 570 nm using a micro-plate reader (Biotek, Winooski, VT, USA).

2.5. Determination of alkaline phosphatase (ALP) activity

MC3T3-E1 cells (3×10^4 cells/mL) were seeded on MATRIGEL™ in 24-well plate and grown for 10 days. Afterwards, the cells were rinsed with ice-cold 1× PBS and incubated for 30 min at room temperature in ALP assay buffer (1.5 M of Tris-HCl [pH 9.0], 1 mM $ZnCl_2$, and 1 mM $MgCl_2$) containing 1% (vol/vol) Triton X-100. Cell extracts were collected, centrifuged, and used for an enzyme assay. ALP activity was determined by using 5 mM of *p*-nitrophenyl-phosphate (*p*NPP) as a substrate. The result is expressed as nanomoles of products formed per minute per milligrams of protein. Protein amount was determined by Lowry's method as modified by Hartree [12].

2.6. Western blot

Osteoblasts were lysed using a Lysis-Cocktail [50 mM Tris, tris(hydroxymethyl)aminomethane–HCl (pH 7.4), 1% (vol/vol) Tween 20, 0.25% sodium deoxycholate, 150 mM NaCl, 1 mM EGTA (ethylene glycol tetraacetic acid), 1 mM O-Vanadate, 1 mM NaF, plus protease inhibitors (1 μg/mL aprotinin, 10 μg/mL leupeptin, and 1 mM 4-(2-aminoethyl)-benzolsulfonyl-fluoride-hydrochloride)] and kept on ice for 2 h, as described previously [13,14]. After clearing the lysate by centrifugation,

the amount of protein obtained was determined using Lowry's method as modified by Hartree [12]. Afterwards, an equal volume of 2× sodium dodecyl sulfate (SDS) gel loading buffer (100 mM Tris-HCl [pH 6.8], 200 mM dithiothreitol [DTT], 4% SDS, 0.1% bromophenol blue, and 20% glycerol) was added to samples, which were then boiled for 5 min. Proteins were resolved by SDS-polyacrylamide gel electrophoresis (SDS-PAGE) and transferred to PVDF membranes. Then, membranes were blocked with either 1% fat-free dried milk or bovine serum albumen (2.5%) in 1× Tris-buffered saline (TBS)–Tween 20 (0.05%, vol/vol) and incubated overnight at 4 °C with appropriate primary antibody at 1:1000 dilutions. After washing in 3× TBS-Tween 20, membranes were incubated with horseradish peroxidase-conjugated anti-rabbit, anti-goat or anti-mouse IgGs antibodies, at 1:2000 dilutions (in all immunoblotting assays), in blocking buffer for 1 h. After washing in 3× TBS, the detection was performed by using enhanced chemiluminescence (ECL). In order to measure the Shh secreted to ECM compartment, the conditioned medium was collected and subjected to Amicon® Ultra-0.5 device (Millipore, NL), exactly as recommended by the manufacturer. Afterwards, the pooled proteins were resolved into a SDS-PAGE system.

2.7. RT-PCR

Total RNA was isolated from osteoblasts by using the Trizol method (Sigma Zwijndrecht, Netherlands) according to the manufacturer's instructions. cDNA was produced by using Oligo-dT primers (Invitrogen, Breda, Netherlands) in a final volume of 30 μL. A PCR was performed for 35 cycles using a 60-second denaturizing step at 94 °C, 60-second annealing step at 60 °C and a 60-second extension step at 72 °C. The product was loaded on agarose gel and detected using ethidium bromide. β-Actin was used as an internal control.

2.8. Phosphoproteome (peptide array)

Phosphoproteome array analysis was done as described elsewhere [15,16]. Furthermore, the protocol of the kinome array is described in detail on the Website (http://www.pepscan.nl/pdf/Manual%20PepChip%20Kinase%200203.pdf). Briefly, osteoblasts were washed in PBS and lysed in a non-denaturing complete lysis buffer. The peptide arrays (Pepscan, Lelystad, The Netherlands), containing up to 1024 different kinase substrates (in triplicate), were incubated with cell lysates for 2 h in a humidified stove at 37 °C plus ^{33}P-g-ATP or ^{33}P-g-ATP (control for non-covalent specific binding) as described earlier. Subsequently, the arrays were washed in 2 M NaCl, 1% Triton-X-100, PBS, 0.1% Tween, and H_2O. Then, arrays were exposed to a phospho-imaging screen for 72 h and scanned on a phospho-imager (Fuji Storm 860, Stanford, GE, USA). The density of the spots was measured and analysed with array software.

2.9. Data analysis of peptide array

For the analysis, clustering using the spearman correlation coefficient was calculated for each combination of sets, and clustering was performed using Johnston hierarchical clustering schemes. For each peptide the average and standard deviation of phosphorylation was determined and plotted in an amplitude-based hierarchical fashion. If only background phosphorylation was present, this amplitude-based distribution can be described by a single exponent. Thus, determining the exponent describing amplitude behaviour of the 500 least phosphorylated peptides should give an adequate description of array background phosphorylation and did so in practice. Peptides of which the average phosphorylation minus 1.96 times the standard deviation was higher than the value expected from describing the background distribution were considered to represent true phosphorylation events. Two-sided heteroscedastic *t*-tests were also performed on each set of values to determine significance ($p < 0.05$).

2.10. Statistical analysis

All experiments were performed in triplicate, and the results shown in the graphs represent the means and standard errors. Cell viability data (assessed by MTT) were expressed as the means ± standard errors of 3 independent experiments carried out in triplicate. Data from each assay were analysed statistically by ANOVA. Multiple comparisons among group mean differences were tested with the Tukey *post hoc* test. Differences were considered significant when the $p < 0.05$. Western blots represent 3 independent experiments. Quantitative expression (RT-PCR) was analysed with Quantity-One software (version: 4.4.0, Bio-Rad).

3. Results

In an effort to understand interaction of the extracellular matrix with the osteoblast compartment, we investigated the effects of a Matrigel™-based scaffold on cell morphology. Contrasting Matrigel™ culture to polystyrene-cultured cells, the MC3T3-E1 pre-osteoblast cells when cultured on polystyrene display the typical morphological features of osteoblasts (Fig. 1a); however, when cultured on Matrigel™-coating (see Material and methods), these cells underwent a morphological transition (Fig. 2a-II), especially when concomitantly exposed to an osteogenic medium (Fig. 1a). Especially prominent were long cytoplasmic protrusions, and at the same time, the cells appeared to lose their proliferative phenotype. The latter notion was confirmed by MTT assays (Fig. 1b) and through analysis of cdk4 and cdk6 expression (Fig. 1c–e). We thus concluded that culturing cells in Matrigel™ provokes a morphological transition.

This hypothesis was confirmed in experiments that assessed the osteogenic functionality of these cells. We determined expression of specific osteoblast housekeeping genes, including osteocalcin (OCN) and alkaline phosphatase (ALP). Both gene products were increased following Matrigel™ culture as evaluated by RT-PCR (Fig. 1f–h). Hence, our differentiation protocol provoked a *bona fide* induction of osteogenesis and not general deregulation of gene expression. Accordingly, ALP activity assays confirmed increased expression of this enzyme in Matrigel™ cultures (Fig. 1k). As osteogenic differentiation involves ECM remodelling, the cathepsin K (CtsK) and B (CtsK) expression was also investigated, but expression of these genes remained unchanged. We concluded that our MATRIGEL™ culture protocol provokes a profound morphological transition in MC3T3-E1 pre-osteoblast cells.

3.1. Generation of kinome profiles

Having established an *in vitro* model that captures morphological transition in osteoblast differentiation, we exploited this situation to characterize comprehensively the associated biochemical changes. The kinome of osteoblast cells were cultured on polystyrene (control group), on basement membrane matrix, or on basement membrane matrix in the presence osteogenic stimulus (osteogenic medium) following 10 days of culture. After incubation of osteoblast lysates on peptide arrays, three identical forms of 976 different kinase substrates occurred in the presence of ^{33}P-γ-ATP efficient phosphorylation, as evident by the incorporation of substantial amounts of radioactivity in the array (Fig. 2a). The technical quality of the profiles was good because the average Pearson product moment correlation coefficient was well in excess of 0.85 between the technical replicas in all experimental groups (Supplementary data, Fig. S1). Thus, the kinome profiles obtained were considered valid, and we decided to analyse the information contained in the data.

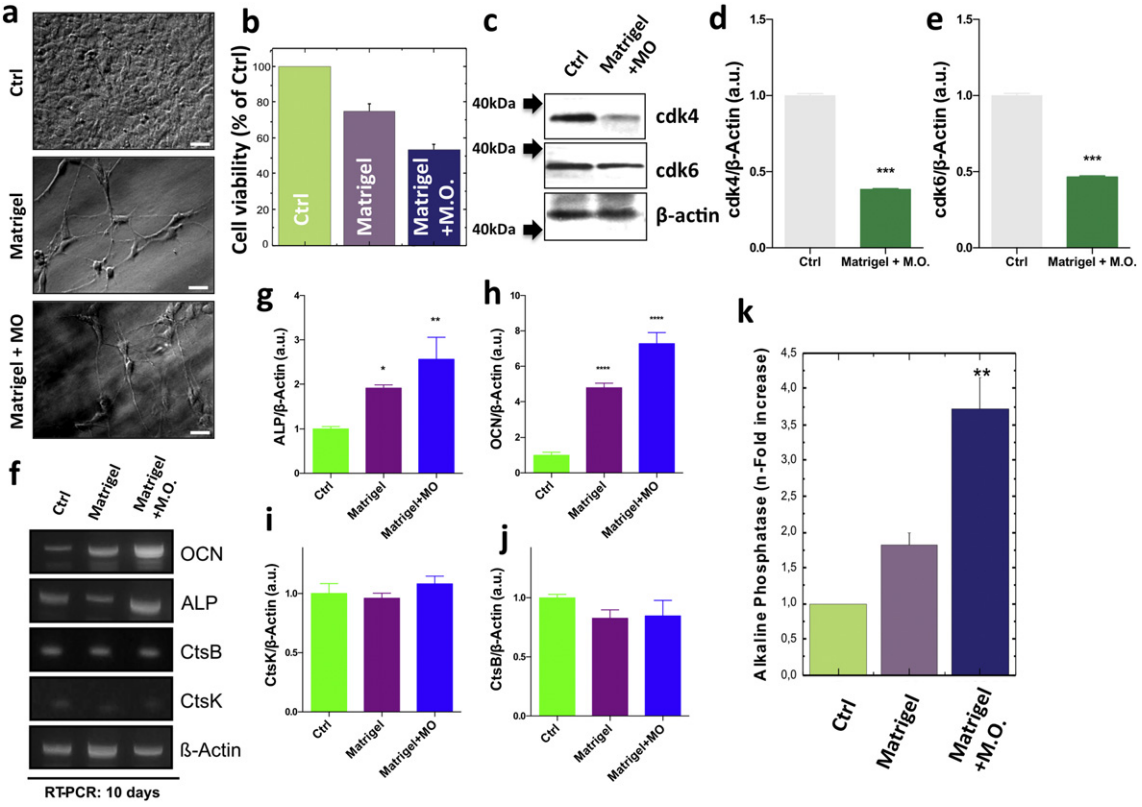

Fig. 1. Effective *in vitro* model for obtaining osteoblast morphological transitions. (a) Morphology presented by MC3T3-E1 pre-osteoblast cells cultured on polystyrene, Matrigel™ or Matrigel™/osteogenic medium (M.O.); (b) cell viability was performed by MTT assay; (c) representative blotting of cdk4 and cdk6; (d) arbitrary data obtained of cdk4 immunoblotting profile; (e) arbitrary data obtained of cdk6 immunoblotting profile; (f–j) classical biomarkers related to bone cells metabolism were expressed in our model *in vitro*; (k) ALP activity assay was performed by using pNPP as substrate. *$p < 0.05$; **$p < 0.003$; ***$p < 0.0001$.

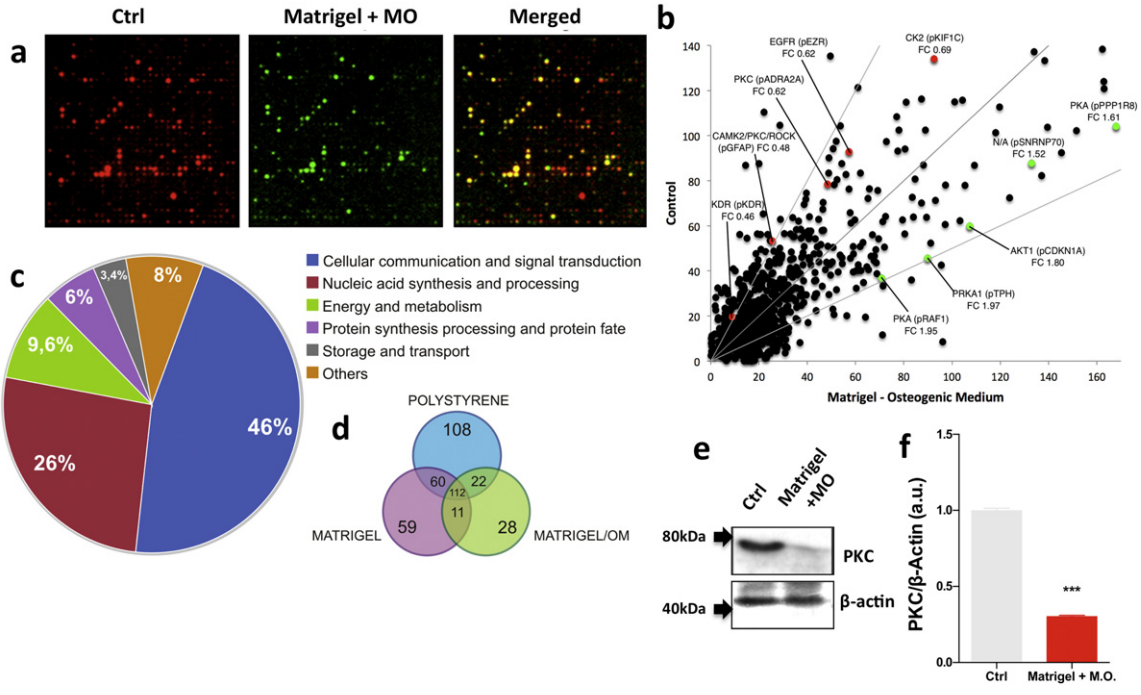

Fig. 2. Generation of kinome profiles of the osteoblast morphological changes. (a) Arrays incorporated substantial amounts of radioactivity, and representative phospho-image scans are shown; (b) median phosphorylation intensity for all 1024 PepChip kinases and substrates. Coloured spots identify areas that presented consistent replicates across PepChip experiments ($p < 0.05$). Red means less phosphorylated (FC < 0.5) and green means more phosphorylated (FC > 1.5) than the control sample. Grey lines represent fold change = 0.5; 1; 2, top to bottom. Spots are identified by the kinase responsible for the phosphorylation event, followed by the phosphorylated substrate (denoted by "p"). FC indicates the individual fold change for each coloured spot; (c) using the gene ontology, these substrates were grouped into cell physiological function; (d) Venn diagram of phosphorylated spots; (e) immunoblotting was used as a validation approach. ***$p < 0.0001$.

3.2. Osteoblast morphological transition is characterized by less diverse and, thus, more singular cellular signal transduction

An initial way of assessing the effects of altered culture conditions on cellular signal transduction using kinome profiles is to analyse the number of significant kinase events, which provides an overall indication of the complexity of cellular signalling. We calculated, for each peptide in our arrays and for each condition, both the average and standard deviation of substrate phosphorylation (a full list of results in Supplementary data - Table S1) and plotted the values obtained in an amplitude-based hierarchical fashion (Supplementary data - Fig. S1a). If only background phosphorylation is present, this amplitude-based distribution can be described by a single exponent (black lines in Supplementary data, Fig. S1b). Peptides of which the average phosphorylation minus 1.96 times the standard deviation is in excess of the value expected from the function describing the background distribution are considered to represent true phosphorylation events. A logarithmic expression of the relative effect for proteins with altered phosphorylation depending on the culture condition is also provided in the Supplementary data (Supplementary data, Fig. S2).

This analysis indicated that osteoblast morphological transition is accompanied by a substantial down regulation of cellular signalling diversity: lysates generated from control cultures phosphorylate 302 unique peptide-substrates, whereas lysates obtained from cells grown on Matrigel™ phosphorylate 242 unique substrates. Additionally, exposing osteoblasts cultured on Matrigel™ to osteogenic medium resulted in cultures that upon lysis phosphorylated only 173 substrates. Thus, morphological transition of osteoblasts is accompanied by less diverse signal transduction, which indicates the emergence of a predominance of very specific signal transduction pathways upon morphological transition.

Construction of Venn diagrams and subsequent calculation of Pearson product-moment of the individual kinome profiles show clustering of results according to the experimental groups (Fig. 2d). The Pearson product-moment is very similar when polystyrene-grown cultures were compared to Matrigel™-grown conventional medium cultures or when Matrigel™-grown conventional medium cultures were compared to Matrigel™-grown osteogenic medium cultures (Supplementary data, Fig. S1). Hence, the results appear to reflect a genuine reduction in cellular signalling. The reduced kinase activity in osteoblast cultured on basement membrane matrix may well be a reflection of their reduced metabolic functionality.

3.3. A phosphoproteome associated to osteoblast morphological transition

Subsequently, we aimed to identify the exact cellular pathways associated with morphological transition. Kinome profiling results were mapped back to the responsible kinases. In the description of the results, the phosphorylated state is denominated by attaching the prefix "p", whereas "FC" indicates the individual fold change for each coloured spot (Fig. 2b). Our analysis revealed that 84 substrates exhibited significantly ($p < 0.05$) differential phosphorylation by lysates obtained cultures with an alternative morphological aspect. An exploration of the gene ontology of those substrates with respect to cell physiological function is shown (Fig. 2c) and provides further insight into the pathways affected by osteoblast morphological change.

Specifically, our results showed that osteoblast morphological transition involves down-regulation of cell cycle-related kinases (cdc2/cdk2 and never in mitosis gene A-related kinase 2), in apparent agreement with the observed cell cycle arrestment (Fig. 1b–e). Fig. 3a summarizes the major findings. Unsurprisingly, in view to the drastic morphological changes observed, kinases involved cytoskeletal remodelling, such as when Src kinases appeared differentially active in the different experimental conditions, which was confirmed when Src activity

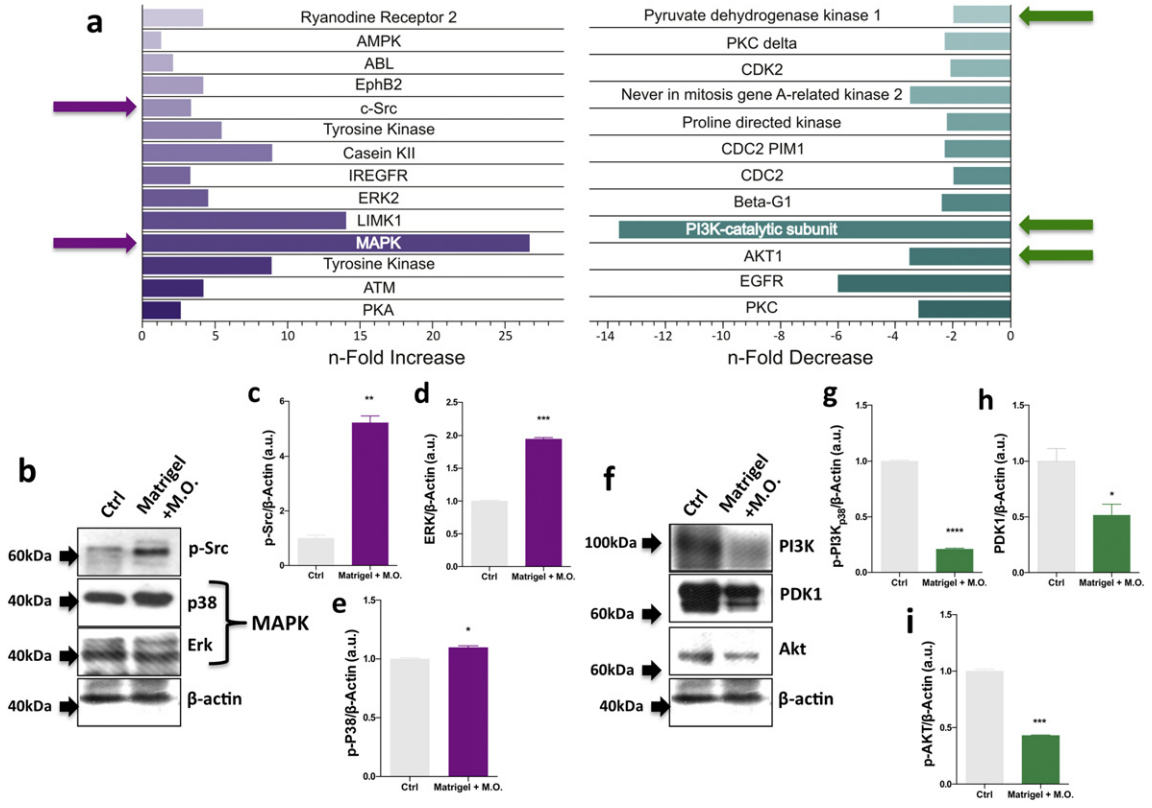

Fig. 3. Modulation of critical kinases was identified in the profiles. (a) Substrates were grouped with respect h-fold increase and n-fold decrease; the results from peptide array were confirmed using conventional technology (b–i). Representative blotting of Src, MAPKs, PI3K, PDK1, AKT, and β-Actin; graphs "c–e" and "g–i" represent arbitrary values obtained by densitometric analysis of the bands normalized by the average values of the respective β-Actin bands. β-Actin was used as loading sample (approximately 75 μg of protein per race). *$p < 0.05$; **$p < 0.0012$; ***,****$p < 0.0001$.

was probed using conventional technology (Fig. 3b,c). Other relevant effects include differential PKA and calcium signalling (RyR receptor) and an increase in MAP kinase signalling (Fig. 3b,d,e). Additionally, a very striking effect is the down-regulation of the PI3kinase/protein kinase B (Akt) pathway (Fig. 4a). As this signalling cassette mediates survival signalling, this effect may be linked to the propensity of Matrigel-challenged cells to enter into apoptosis (Fig. 3f–i).

Further insight was generated through the construction of interactomes, which revealed alternative activation in the experimental groups of SHP2-mediated signalling (Supplementary data, Fig. S5), retinoblastoma protein-associated events (Fig. 4b), regulation of nuclear SMAD2/3 signalling (Supplementary data, Fig. S4), and the c-MYB transcription factor network (Supplementary data, Fig. S3). The constructed interactomes demonstrate a strong FoxO signal associated with the osteoblast morphological transition (Fig. 4a), which was confirmed when FoxO was probed using conventional technology (Fig. 4c–f).

Upon further inspection of the data, a strong hedgehog fingerprint emerged. In general, non-canonical hedgehog signalling leads to dendrite extension and is accompanied by the activation of Src-like kinases, LIMK, p42/p44 MAP kinase, and p38 MAP kinase [20–22], which were all evident in the profiles. Classical Hh signalling involves modulation of GSK-3β and PKA as well as casein kinase, which were all also clearly visible in the profiles. As seen in the PepChip, the critical kinase for canonical hedgehog signalling fused [23], and became less active as, assayed by phosphorylation of FPDQAYANSQP, a peptide corresponding to its autophosphorylation site (of which deactivation is necessary for hedgehog signalling). These changes prompted us to investigate the involvement of hedgehog signalling during osteoblast morphological transition.

3.4. A requirement for hedgehog signal transducers during osteoblast morphological transition

The notion that Shh signalling is implicated in morphological transition of osteoblasts was confirmed in experiments that evaluated the expression of the hedgehog receptor Patched (PTCH), and hedgehog-signalling transcription factors Gli1 and Gli-3. Both PTCH and Gli1 were upregulated when osteoblasts were cultured onto Matrigel™ for ten days (Fig. 5a,b). In parallel experiments, we collected the conditioned medium in order to investigate possible Shh released into the extracellular compartment. Our results showed a significant release of Shh (Fig. 5c,d), which suggests that osteoblast morphological transition involves activation of autocrine Shh signalling. Fig. 5e summarizes Shh signalling involvement during osteocyte-like early differentiation requiring FoxO expression.

3.5. Hedgehog signalling is both sufficient and necessary for the morphological change of osteoblast

Prompted by the above-described results, we decided to assess the actual importance of hedgehog signalling for the osteoblast morphological transition. To this end, either we experimentally abrogated Hedgehog signalling, using the smoothened inhibitor cyclopamine [24], or we artificially enhanced hedgehog signalling, *via* the addition of recombinant Hedgehog. Morphologically, the hedgehog inhibitor cyclopamine clearly impaired the ability of MATRIGEL™ and/or osteogenic medium to provoke evident morphological change (Fig. 6a), whereas forced induction of hedgehog signalling enhanced this phenotype of osteoblasts (Fig. 6a). Biochemically, cyclopamine prevented exit from the cell cycle,

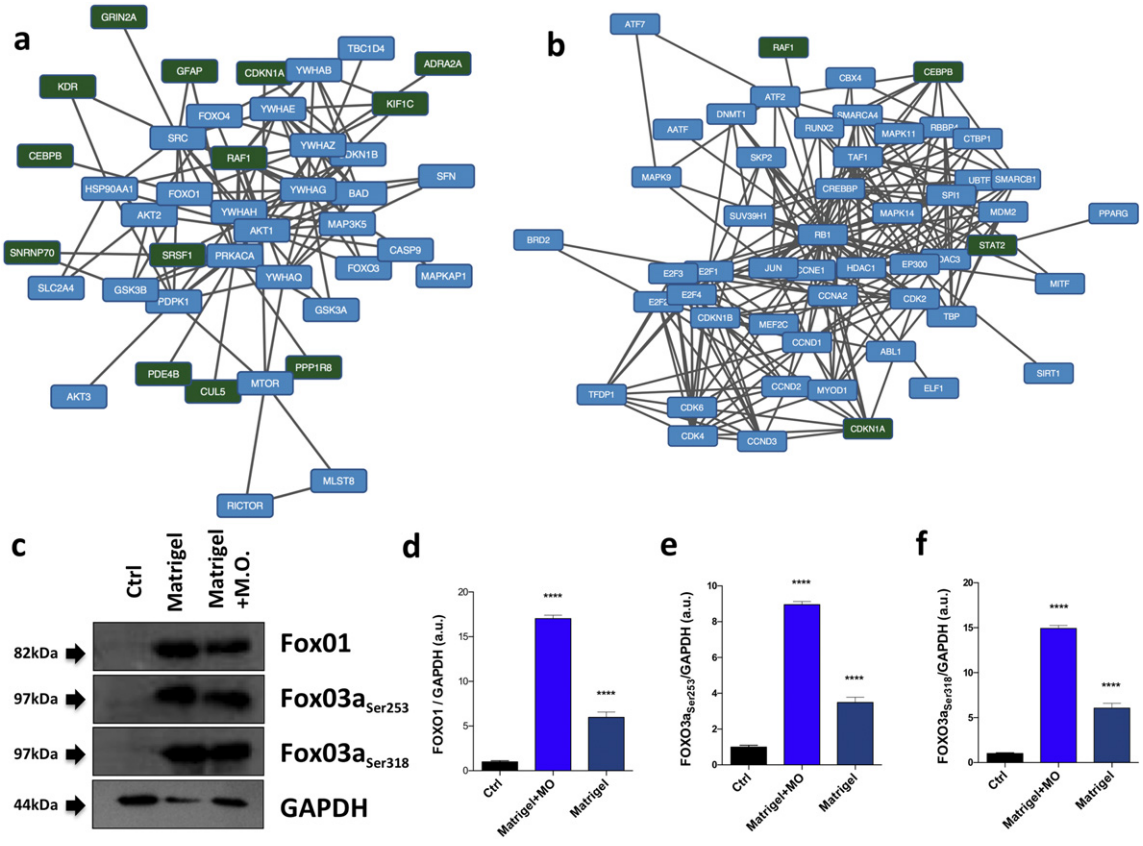

Fig. 4. Interactomes from phosphoproteome analysis suggest FoxO (a) and retinoblastoma (b) requirements. These interactomes were extracted from the NCI-Pathway Interaction Database [17] as relevant for the list of proteins with altered phosphorylation profiles ($p < 0.05$); Proteins from the list are highlighted in green. Proteins are represented by gene names. The network was generated by Cytoscape 3.1.1 [18] with the Jepetto plugin [19]. As interactomes suggested FoxO involvement, we decided to validate this by exploring Western blot and (c) brings representative blots for FoxO1, phospho-FoxO3a (Ser253), phospho-FoxO3a (Ser318); (d–f) arbitrary data obtained from the densitometry analysis of the bands normalized by the average values of the respective GADPH bands. Significance was considered when ****$p < 0.0001$.

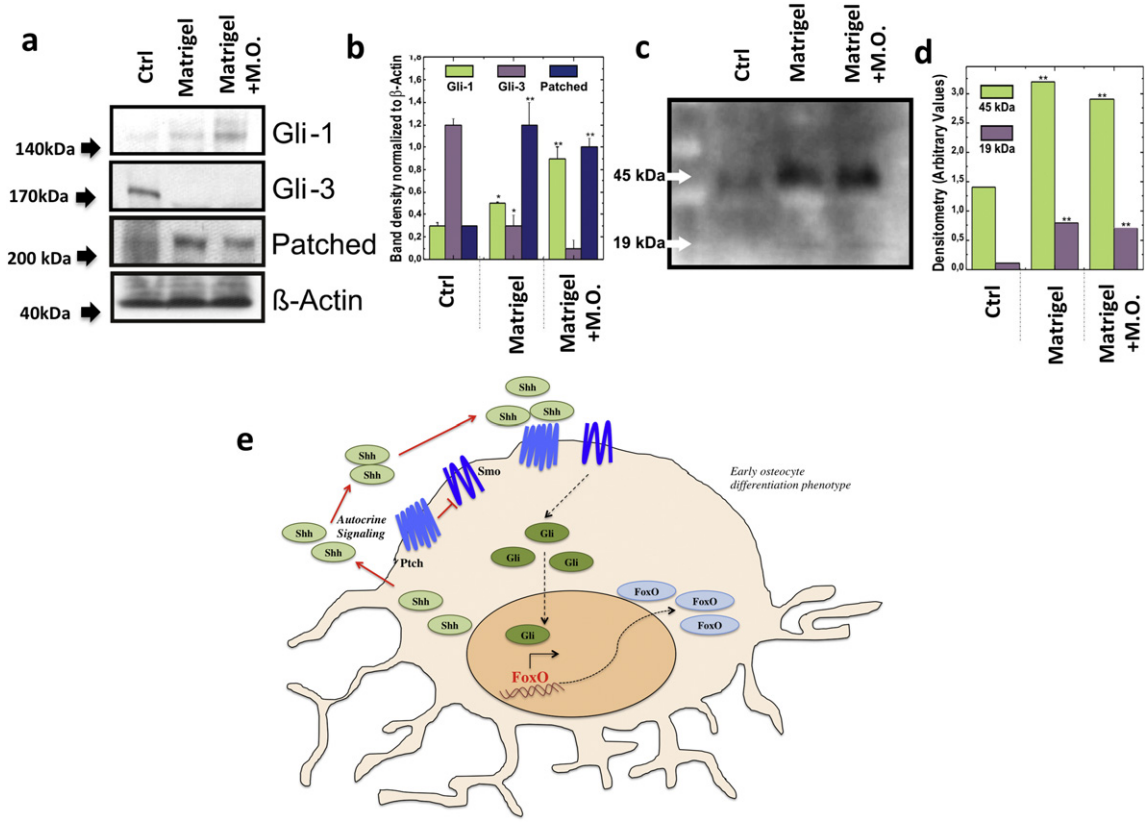

Fig. 5. Hedgehog signalling members during osteoblast morphological transition. (a) Representative blots of Patched, Gli-1, and Gli-3 during the osteoblast morphological change transition; (b) graph brings arbitrary values obtained from densitometry analysis of the bands (Patched, Gli-1, and Gli-3); (c) Shh released to extracellular compartment, as it was measured in concentrated conditioned media; (d) graph brings arbitrary values obtained from densitometry analysis of the bands (released Shh) normalized by the average values of the respective β-Actin bands; (e) general schematization suggesting an autocrine Shh signalling in governing osteocyte-like early differentiation. Significance was considered when *$p < 0.05$; **$p < 0.0001$.

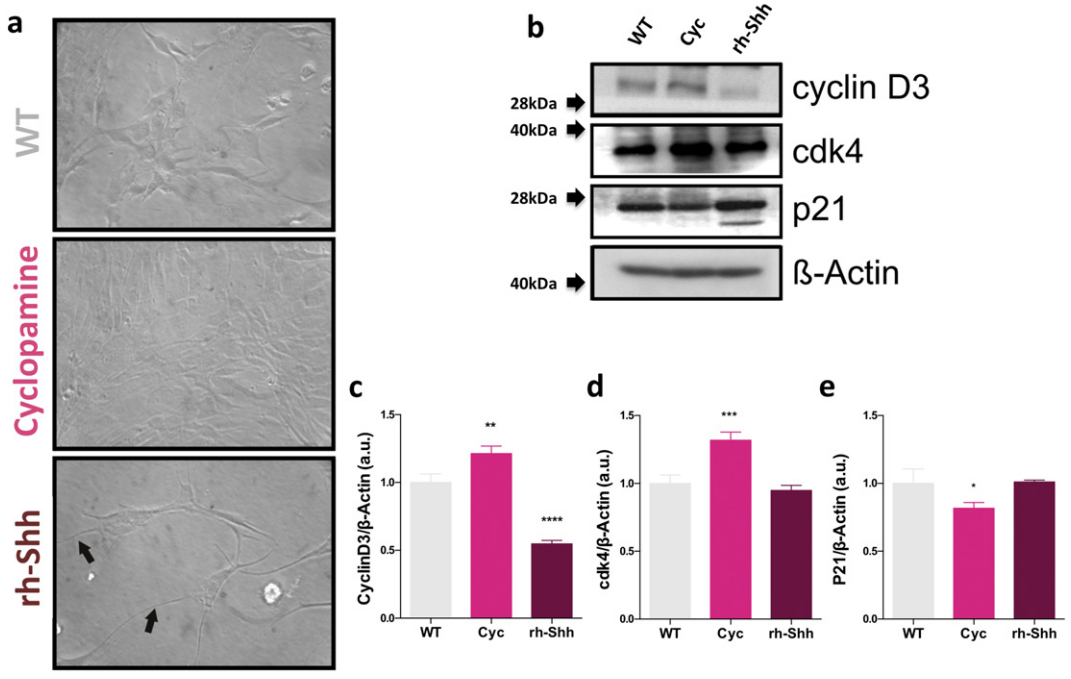

Fig. 6. Hedgehog signalling drives osteoblast morphological transition. (a) Morphologically, the hedgehog inhibitor cyclopamine clearly impaired the ability of MATRIGEL™ and/or osteogenic medium to provoke the significant osteoblast morphological changes; (b) representative blotting of CycliD3, cdk4, p21, and β-Actin. Cyclopamine (Cyc) prevented exit from the cell cycle, as evident from increased activity of cell cycle kinases and significant reduction of cell cycle inhibitor p21 expression. Graphs "c–e" represent arbitrary values obtained by densitometric analysis of the bands normalized by the average values of the respective β-Actin bands. β-Actin was used as loading sample (approximately 75 μg of protein per race). Cyc at the concentration used here was not cytotoxic. *$p < 0.05$; **$p < 0.0012$; ***,****$p < 0.0001$.

as evident by increased activity of cell cycle kinases and reduced expression of the cell cycle inhibitor p21, whereas exogenous hedgehog enhanced the exit of the cell cycle as judged by these parameters (Fig. 6b–e). Overall, our results suggest the importance of Shh signalling during morphological changes of osteoblast.

4. Discussion

Much of the mechanisms responsible for morphological transition up of osteoblast are unclear [25], but increased insight into these mechanisms may open novel rational avenues in regenerative medicine. Here we exploited a Matrigel™-based scaffold as an *in vitro* model system for evaluating osteoblast morphological changes and employed this system to contrast kinome profiles of cultures with an alternative morphological aspect. The results provide a wealth of biochemical data related to morphological transition but especially show an important role of Shh signalling. As we feel the Matrigel™-exposed cultures recapitulate important aspects of osteoblasts *in vivo*, our results should have relevance for understanding the organic architecture of bone.

Most of our results are broadly in line with the contemporary biomedical literature. For instance, a clear activation of the hunger kinase AMPK is noted during osteoblast encapsulation in ECM, and activation of this kinase is a typical response to nutrient deprivation [26–28]. AMPK-associated effects that promote cell energy conservation include reduced glycolysis and diminished protein synthesis through the down-regulation of p70 S6 kinase [29]. In apparent agreement, our kinome profiles found reduced activity of pyruvate dehydrogenase kinase (associated with diminished glycolic activity) linked to osteoblast morphological transition as well as a general down-regulation of metabolism (as judged from the reduced number of significantly above background phosphorylated substrates). The apparent conformity of our results to the existing literature in this respect bolsters confidence in the validity and usefulness of our data.

The modulation of a large number of peptides associated with both canonical and non-canonical hedgehog signalling was very interesting, subsequent analysis revealed that Shh signalling is both necessary as well as sufficient to drive the osteoblast morphological changes. Hedgehog signalling in general has already been implicated in many aspects of osteogenesis and bone physiology: in particular, Ihh signalling is necessary for the formation of osteoblasts and controls bone formation and resorption, also *via* regulating PTHrP and RANKL expression [30]. Our results further highlight the importance of this signalling system in bone physiology.

A qualifier in this respect is that osteoblast morphological transition has not yet been conclusively linked to altered functionality, which may be due to the difficulties in investigating this compartment in general and the osteoblast to osteocyte transition in particular, but is at least not inconsistent with the existing data (*e.g.* the reduced osteolysis seen in aged mice upon inhibition of Hh signalling). Furthermore, one of the most defining morphological characteristics of the osteocyte lineage is the projection of numerous dendrites into the bony matrix, and recently it has emerged that the non-canonical branch of Hh signalling elicits a dendrite extension response in target cells [21,22,31]. Thus, our finding supports that Hh signalling is a cardinal regulator of osteoblast morphological changes. This is in agreement with both the existing insights into bone physiology as well as with the existing ideas regarding the cell biological effects of hedgehog signalling. In general, non-canonical hedgehog signalling leads to dendrite extension and is accompanied by the activation of Src-like kinases, LIMK, p42/p44 MAP kinase, and p38 MAP kinase, which are all evident in the profiles. Classical Hh signalling involves modulation of GSK-3β and PKA as well as casein kinase, which are all clearly visible in the profiles. In agreement, we have previously reported that Ihh is expressed by mature colonocytes and regulates their differentiation *in vitro* and *in vivo*. These data identified a new Wnt-Hh axis in colonic epithelial renewal [32].

Our results seem to indicate a fairly high tendency of osteoblast-acquired new phenotype to undergo apoptosis, especially through down regulation of the important PKB pathway. In nature, it is known that osteocyte compartment is involved in detecting microdamage and subsequently undergoes apoptosis as part of the signals that lead to microdamage repair [33,34], which could explain an apparent high propensity of programmed cell death. On the other hand, osteocytes are also well known to be exquisitely mechanosensitive and in our experimental conditions, no strain is applied to those systems. Hence, the apparent weak survival signalling in the osteoblast-acquired new phenotype compartment, as detected in our experiments, may also be due to a lack of mechanostimulation and further experiments are needed to distinguish between these two notions.

Bio-inspired *in vitro* scaffolds systems allow researchers to investigate global molecular and dynamic interactions between cells and to mimic the surrounding matrix. Disregarding the problem of mechanostimulation, our study recapitulated osteoblast morphological changes *in vitro* and catalogued a functional protein network, identifying hedgehog signal transduction as a critical regulator in the events involved.

Supplementary data to this article can be found online at http://dx.doi.org/10.1016/j.bone.2017.06.012.

Acknowledgements

Grant sponsors CNPq (301966/2015-0, 477452/2012-4) and Fapesp (2014/22689-3). W.F.Z. is supported by CNPq fellowship (PQ-2). AM, RM, RS, CJCF, and WFZ performed the experiments and collected the data. WFZ, CVF, MPP, and JMG supervised the work. AM, WFZ, MPP, and RS wrote the paper. We are indebted to Prof. Anna Teti for her suggestions on this manuscript. All authors reviewed and approved the manuscript. The authors declare no conflict of interest.

References

[1] K.B. Paiva, W.F. Zambuzzi, T. Accorsi-Mendonça, R. Taga, F.D. Nunes, M.C. Sogayar, et al., Rat forming incisor requires a rigorous ECM remodelling modulated by MMP/RECK balance, J. Mol. Histol. 40 (2009) 201–207.
[2] S. Rhee, Fibroblasts in three-dimensional matrices: cell migration and matrix remodelling, Exp. Mol. Med. 41 (2009) 858–865.
[3] W.F. Zambuzzi, C.L. Yano, A.D. Cavagis, M.P. Peppelenbosch, J.M. Granjeiro, C.V. Ferreira, Ascorbate-induced osteoblast differentiation recruits distinct MMP-inhibitors: RECK and TIMP-2, Mol. Cell. Biochem. 322 (2009) 143–150.
[4] M.H. Kural, K.L. Billiar, Regulating tension in three-dimensional culture environments, Exp. Cell Res. 319 (2013) 2447–2459.
[5] A.C. de Oliveira Demarchi, W.F. Zambuzzi, K.B. Paiva, M.D. da Silva-Valenzuela, F.D. Nunes, R. de Cássia Sávio Figueira, et al., Development of secondary palate requires strict regulation of ECM remodelling: sequential distribution of RECK, MMP-2, MMP-3, and MMP-9, Cell Tissue Res. 340 (2010) 61–69.
[6] K. Parikh, M.P. Peppelenbosch, S. Johnson, T. Hunter, G. Manning, D. Whyte, R. Martinez, T. Hunter, S. Sudarsanam, R. Stoughton, S. Friend, H. Versteeg, E. Nijhuis, et al., Kinome profiling of clinical cancer specimens, Cancer Res. American Association for Cancer Research 70 (2010) 2575–2578, http://dx.doi.org/10.1158/0008-5472.CAN-09-3989 (cited 2016 Jun 20).
[7] H. Zhu, M. Snyder, Protein arrays and microarrays, Curr. Opin. Chem. Biol. 5 (2001) 40–45, http://dx.doi.org/10.1016/S1367-5931(00)00170-8.
[8] S. Gemini-Piperni, R. Milani, S. Bertazzo, M. Peppelenbosch, E.R. Takamori, J.M. Granjeiro, et al., Kinome profiling of osteoblasts on hydroxyapatite opens new avenues on biomaterial cell signaling, Biotechnol. Bioeng. 111 (2014) 1900–1905.
[9] S. Gemini-Piperni, E.R. Takamori, S.C. Sartoretto, K.B. Paiva, J.M. Granjeiro, R.C. de Oliveira, et al., Cellular behavior as a dynamic field for exploring bone bioengineering: a closer look at cell-biomaterial interface, Arch. Biochem. Biophys. 561 (2014) 88–98.
[10] R. Milani, C.V. Ferreira, J.M. Granjeiro, E.J. Paredes-Gamero, R.A. Silva, G.Z. Justo, et al., Phosphoproteome reveals an atlas of protein signalling networks during osteoblast adhesion, J. Cell. Biochem. 109 (2010) 957–966.
[11] T. Mosmann, Rapid colorimetric assay for cellular growth and survival: application to proliferation and cytotoxicity assay, J. Immunol. Methods 65 (1983) 55–63.
[12] E.F. Hartree, Determination of proteins: a modification of Lowry method that give a linear photometric response, Anal. Biochem. 48 (1972) 422–427.
[13] M. Bispo de Jesus, W.F. Zambuzzi, R.R.R. Sousa, C. Areche, A.C.S. Souza, H. Aoyama, et al., Ferruginol suppresses survival signaling pathways in androgen-independent human prostate cancer cells, Biochimie 90 (2008) 843–854.
[14] K.C. de Souza Queiroz, W.F. Zambuzzi, A.C. Santos de Souza, R.A. da Silva, D. Machado, G.Z. Justo, et al., A possible anti-proliferative and anti-metastatic effect of irradiated riboflavin in solid tumours, Cancer Lett. 258 (2007) 126–134.

[15] J.W. van Baal, S.H. Diks, R.J. Wanders, A.M. Rygiel, F. Milano, J. Joore, J.J. Bergman, M.P. Peppelenbosch, K.K. Krishnadath, Comparison of kinome profiles of Barrett's esophagus with normal squamous esophagus and normal gastric cardia, Cancer Res. 66 (24) (2006 Dec 15) 11605–11612.
[16] S.H. Diks, K. Kok, T. O'Toole, D.W. Hommes, P. van Dijken, J. Joore, M.P. Peppelenbosch, Kinome profiling for studying lipopolysaccharide signal transduction in human peripheral blood mononuclear cells, J. Biol. Chem. 279 (2004) 49206–49213.
[17] C.F. Schaefer, K. Anthony, S. Krupa, J. Buchoff, M. Day, T. Hannay, PID: the Pathway Interaction Database, Nucleic Acids Res. 37 (2009) D674–D679.
[18] G. Su, J.H. Morris, B. Demchak, G.D. Bader, Biological network exploration with cytoscape 3, Curr. Protoc. Bioinforma. Ed. Board Andreas Baxevanis Al 47 (2014) 8.13.1–8.13.24.
[19] C. Winterhalter, P. Widera, N. Krasnogor, JEPETTO: a Cytoscape plugin for gene set enrichment and topological analysis based on interaction networks, Bioinformatics Oxford England 30 (2014) 1029–1030.
[20] M.F. Bijlsma, K.S. Borensztajn, H. Roelink, M.P. Peppelenbosch, C.A. Spek, Sonic hedgehog induces transcription-independent cytoskeletal rearrangement and migration regulated by arachidonate metabolites, Cell. Signal. 19 (12) (2007 Dec) 2596–2604.
[21] M.F. Bijlsma, M.P. Peppelenbosch, C.A. Spek, H. Roelink, Leukotriene synthesis is required for hedgehog-dependent neurite projection in neuralized embryoid bodies but not for motor neuron differentiation, Stem Cells 26 (2008) 1138–1145.
[22] M.F. Bijlsma, M.P. Peppelenbosch, C.A. Spek, H. Roelink, Leukotriene synthesis is required for hedgehog-dependent neurite projection in neuralized embryoid bodies but not for motor neuron differentiation, Stem Cells 26 (5) (2008 May) 1138–1145.
[23] P.P. Thérond, J.D. Knight, T.B. Kornberg, J.M. Bishop, Phosphorylation of the fused protein kinase in response to signaling from hedgehog, Proc. Natl. Acad. Sci. U. S. A. 93 (9) (1996 Apr 30) 4224–4228.
[24] K.C. Queiroz, C.A. Spek, M.P. Peppelenbosch, Targeting hedgehog signaling and understanding refractory response to treatment with hedgehog pathway inhibitors, Drug Resist. Updat. 15 (4) (2012 Aug) 211–222.
[25] E.M. Aarden, E.H. Burger, P.J. Nijweide, Function of osteocytes in bone, J. Cell. Biochem. 55 (1994) 287–299.
[26] B. Dasgupta, J.S. Ju, Y. Sasaki, X. Liu, S.R. Jung, K. Higashida, et al., The AMPK β2 subunit is required for energy homeostasis during metabolic stress, Mol. Cell. Biol. 32 (2012) 2837–2848.
[27] W.N. Hait, M. Versele, J.M. Yang, Surviving metabolic stress: of mice (squirrels) and men, Cancer Discov. 4 (2014) 646–649.
[28] E.E. Vincent, P.P. Coelho, J. Blagih, T. Griss, B. Viollet, R.G. Jones, Differential effects of AMPK agonists on cell growth and metabolism, Oncogene 34 (2015) 3627–3639.
[29] Y.M. Yang, C.Y. Han, Y.J. Kim, S.G. Kim, AMPK-associated signaling to bridge the gap between fuel metabolism and hepatocyte viability, World J. Gastroenterol. 16 (2010) 3731–3742.
[30] K.K. Mak, Y. Bi, C. Wan, P.T. Chuang, T. Clemens, M. Young, Y. Yang, Hedgehog signaling in mature osteoblasts regulates bone formation and resorption by controlling PTHrP and RANKL expression, Dev. Cell 14 (2008) 674–688.
[31] M.F. Bijlsma, C.A. Spek, M.P. Peppelenbosch, Hedgehog: an unusual signal transducer, Bioessays 26 (2004) 87–394.
[32] G.R. van den Brink, S.A. Bleuming, J.C. Hardwick, B.L. Schepman, G.J. Offerhaus, J.J. Keller, et al., Indian hedgehog is an antagonist of Wnt signaling in colonic epithelial cell differentiation, Nat. Genet. 36 (2004) 277–282.
[33] A. Del Fattore, A. Teti, N. Rucci, Bone cells and the mechanisms of bone remodelling, Front. Biosci. (Elite Ed.) 4 (2012) 2302–2321.
[34] A. Teti, A. Zallone, Do osteocytes contribute to bone mineral homeostasis? Osteocytic osteolysis revisited, Bone 44 (1) (2009) 11–16.